WM35

19th International Symposium of Ballistics, 7–11 May 2001, Interlaken, Switzerland

SHAPED CHARGE JET BREAK-UP TIME FORMULA CONFIRMED

Eitan Hirsch and Dan Mordehai

IDF, MIL P.O. Box 02128 Israel

SCAN, a semi-analytical code for analyzing shaped charges [2–4], takes into consideration the fact that when the liner of a cylindrically symmetric shaped charge collapses, its thickness profile becomes wedge like (Fig. 1). This phenomenon very significantly influences the formed jet parameters. (The effect is calculated in the Brigs code as well [18]) The break-up time, (Eq. (1)), as used in the SCAN code, shows a very good agreement to experimental data. In [5] by increasing the liner thickness T_L the V_{pl} parameter is found to increase. In this paper, we propose an interpretation for the jet break-up time formula using the Strength Failure Surface (SFS) model [6]. Shear bands are formed in the liner material at the SFS when it enters the collision region, in a process that is described in some detail. They are called the primary set of shear bands. The dependence of V_{pl} on the liner thickness is shown to relate to the elastic deformation that prevails upon these shear-bands' formation. A secondary set of shear bands is formed when the jet just begins to elongate. The lengths of these secondary shear bands sum up to the initial jet diameter times $\sqrt{2}$ prior to the final jet break-up stage, which explains Eq. 1.

INTRODUCTION

Equation 1 [1] states that the break-up time, t_B, of the shaped charge jet is equal to the initial diameter of the elongating jet d_{in} divided by the average velocity difference, V_{pl}, between neighboring segments that the jet breaks into:

$$t_B = \frac{d_{in}}{V_{pl}} \tag{1}$$

This formula was found in 1979, using a computer code based on the very simplified P.E.R. model [7]. It was then reconfirmed in 1984 in a series of experiments where great care was taken in the analysis to avoid errors that might rise by the use of this model and errors stemming from simplifying assumptions made in the code [8]. Still applications were later found where it was necessary to vary the value of the V_{pl} parameter in order to fit new data obtained in experiments where exotic liners were used, especially when the liner thickness was not constant [9].

In a recently reported series of experiments [5] the V_{pl} value and the accumulated length were measured for the same shaped charge design, using liners made of identical copper material but in five different thickness values. The results are quoted in Table 1.

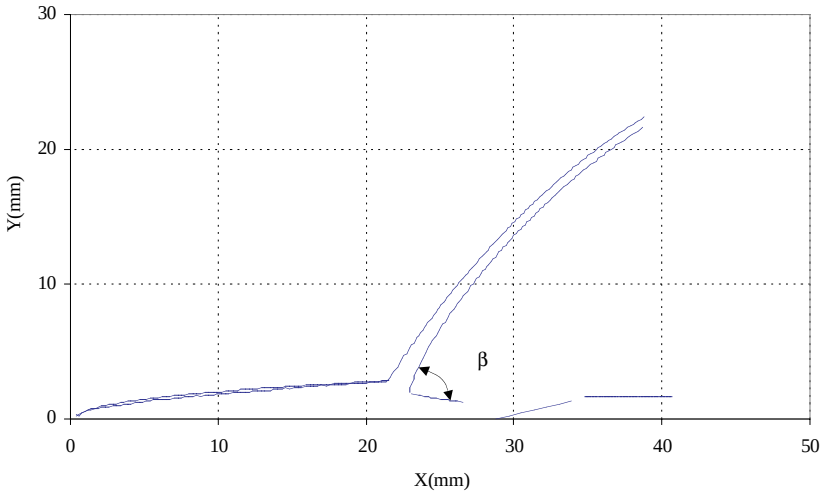

Figure 1: Profile of the collapsing 0.6 mm liner when explosion wave front arrives at the liner base.

When compared to the SCAN code using the V_{pl} measured values the calculated accumulated length of the jets were reproduced with an excellent agreement. The cases of the most commonly used liner thickness (1 mm) the thinnest (0.4 mm) and the thickest that still forms a jet long enough for good comparison (1.9 mm) are depicted in Fig. 2.

The agreement between the experimental results and Eq. (1) for such a wide range of values of T_L and V_{pl}, when the liner thickness is constant for each shot is excellent. It hints to the possibility that the need to make V_{pl} varying as a function of the jet origin along the liner rises from sharp changes of conditions along the liner directrix. This in fact was the reason for the extension of Eq. (1) in [9].

SHEAR BAND FORMATION AT THE SFS

The Strength Failure Surface (SFS) during jet formation by a collapsing liner is shown in Fig. 3, using the Lagrange processor simulation by the Autodyn-2D code. (Note the small angle between the SFS and the axis of symmetry formed because the pressure is higher on the jet forming side than on the other side). The value of the maximum deformation energy that the liner material dissipates (denoted as E_d) was chosen for this demonstration run example to be 100 Joul/cc.

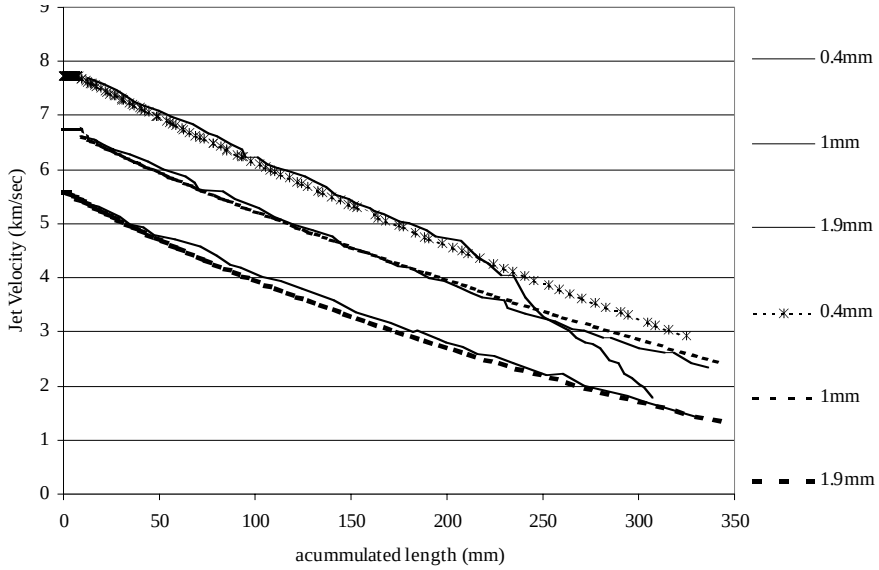

Fig. 2: Ref. [5] Data – solid lines compared to scan predictions – dashed lines.

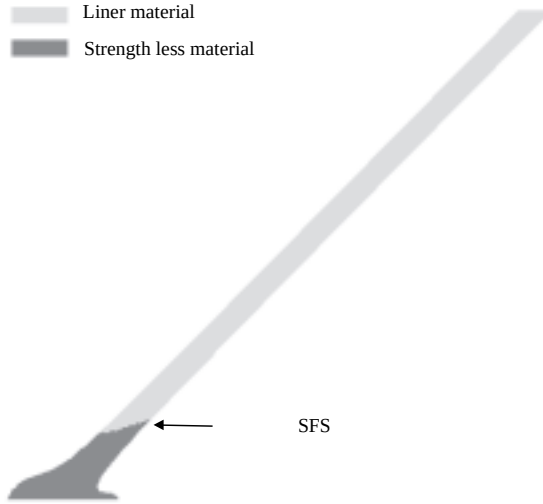

Fig. 3: The SFS in the liner for assumed 100 Joul dissipation energy.

The above description assumes that there exists a continuous flow of material over the SFS strength discontinuity namely the loss of strength is a continuous process. This assumption is convenient for the code run but is in fact artificial. In reality, following a shear band formation at the SFS, a release of tension occurs [17]. The material at the SFS thus flows forward some distance dS becoming deformed again, until a new shear band forms at distance dS behind this front. That process slices the incoming material by for-

ming the next shear band, thus bringing the flow back to the original state. This is a "pulsating" mechanism that results from the fact that upon a shear band formation the tension is temporarily released and time is needed to rebuild it. Let's denote the strain rate at the SFS as η and the elastic deformation of the material leading to shear band formation as ε. Then the recovery-time after each tension release that follows a shear band formation is given by ε/η. Multiplying this time by the liner's radial collapse velocity:

$$V_r = V_f \sin\beta \tag{2}$$

(where V_f is the flow velocity and β is the collapse angle) yields the expected distance between neighboring shear bands:

$$dS = V_r \frac{\varepsilon}{\eta} \tag{3}$$

THE DISTANCE BETWEEN NEIGHBORING SHEAR BANDS

We calculate the length along the directrix that corresponds to one average segment for all the three liners referred to in Fig. 2 and represent it as a function of V_r assuming V_{pl} were 85 m/sec for all the three liners (Fig. 4). Then we find that this length (denoted L_p) becomes independent of the liner thickness apart from the regions where the jet tip particle is formed and at the far tails. Thus, if we use the real V_{pl} value for each liner thickness then the value of L_p for a given V_r is proportional to V_{pl}.

We know from statistical analysis of the jet-particles [10] that each jet segment corresponds on the average to four shear bands. The distance between neighboring shear bands is thus equal to:

$$dS = \frac{L_p}{4} \tag{4}$$

in the jet velocity region where the measurements were taken namely not including the far tails. The kinetic energy lost at the material between an already formed shear band and the next to form, is thus given by the expression: $1/2\rho\cdot(1/4V_{pl})^2$ while the elastic energy released in the shear band formation is: $1/2\rho C^2\varepsilon^3$ where C is the sound velocity in the liner material. Comparing these expressions we find that:

$$\varepsilon = \frac{V_{pl}}{4C} \tag{5}$$

Using C = 4000 m/sec for copper the value of ε for the above liners is also given in Table 1, as well as the respective stress.

We find from Eq. (3) that this calculation is consistent with the assumption that the strain rate in compression is proportional to V_r.

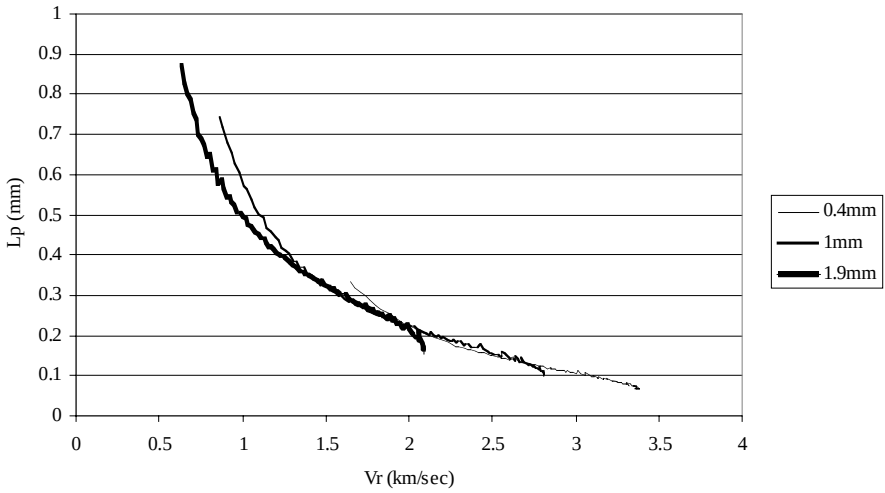

Fig. 4: The length along the directrix per one average segment vs. the radial collapse velocity.

Table 1. – Dependence of V_{pl} on the liner thickness for 60 degrees opening angle 45 mm charge diameter, point initiated 65/35 RDX/TNT shaped charge. Quoted from ref. 5 & corresponding calculated values of elastic strain and stress at shear bands formation.

Liner thickness (mm)	Measured V_{pl} (meters/sec)	Calculated ε	Calculated stress (Kbar)
0.4	77	0.0048	6.9
0.6	80	0.0050	7.2
1.0	85	0.0053	7.6
1.9	105	0.0066	9.4
3.0	140	0.0088	12.6

The values of ε found indicate that the elastic deformation at shear band formation is few times larger than the static yield strain. The corresponding stress, $\rho C^2\varepsilon$, is accordingly larger than the static yield stress but still considerably less than the tension of 18 to 24 kbars required for scabbing of the material (see Appendix). This is expected, because the material must have a considerable excess of free elastic energy in order to break through the grains when forming a macroscopic shear band but still needs much less free energy than at the scabbing threshold.

THE INTERNAL TUBES STICKING TOGETHER

In the jet, the shear bands form the outer and inner boundaries of the concentric tubes that form the jet [11]. These tubes are in motion relatively to each other during most of the jet elongation [11, 12]. Each shear band ends on the formed jet free outer surface. The location of this end initiates the beginning of a break.

As long as the inertial motion overcomes the material forces it delays the break-up process. With ongoing time, the relative slide velocity between neighboring tubes slows down however. The shear bands, initially at much higher temperature than that inside the tubes' material, cool by conducting their heat to the tubes, making the temperature inside the whole jet material more homogeneous. Finally the tubes stick together [12] and the break-up process enters its final phase and completes.

As the internal tubes within the jet begin to elongate when the jet forms, they develop their own secondary set of shear bands that allows them to elongate. These shear bands form at 45° to the axis of symmetry, not only as shown in [13] but through their thickness as well (see Fig. 5). These shear bands, formed at the beginning of the jet elongation keep their length crossing through the tube thickness direction unchanged. As the tubes stick together the secondary shear bands join to form continuous macroscopic shear bands through the full thickness of the jet. By the end of this sticking together of the tubes these shear bands' absolute lengths eventually accumulates to d_{in} times $\sqrt{2}$.

As mentioned above, the slide motion of the secondary shear bands directed at 45° to the tubes' thickness starts at the beginning of the jet elongation. Their slide velocity reached at the break-up stage has on the average an axial component equal to V_{pl}. Since their shear lengths component in the axial direction accumulate to d_{in}, the result of Eq. (1) is obtained.

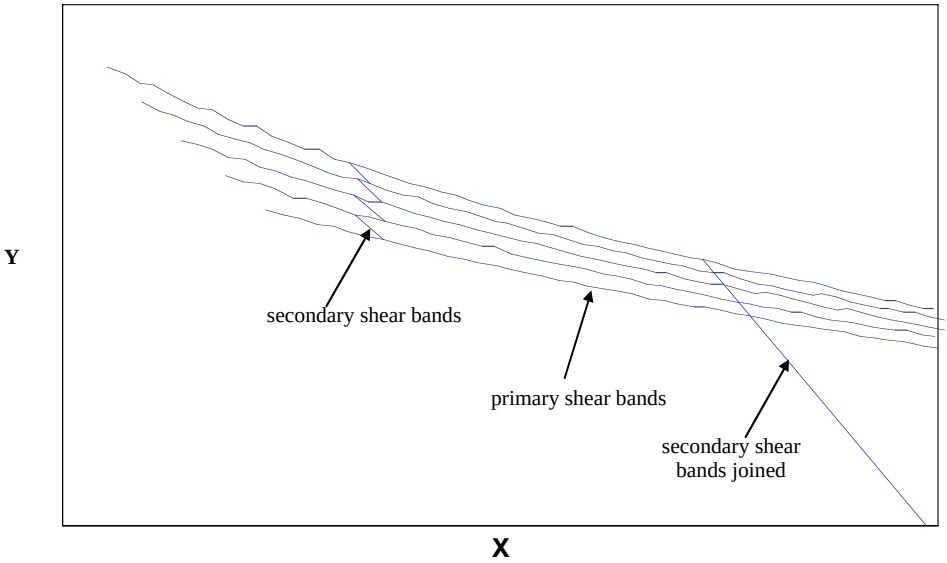

Fig. 5: Schematic illustration of the internal tubes and how their secondary shear bands join to form long shear bands that slide until final break-up is reached.

SUMMARY

Unlike the break-up process of expanding rings and shells of bombs, the shaped charge jet material becomes sliced with a primary set of shear bands similar to those observed in the heads of retrieved rods for kinetic energy penetration [14]. This set (also observed in [13]) determines the potential breakup locations along the jet. There are four shear bands per particle on the average [10,15,16]. The value of the V_{pl} parameter is related to the peak elastic strain of the liner material at shear bands formation (ε). The higher ε, the larger the distance is between neighboring shear bands and also the larger V_{pl} becomes. In thin liners, ε is small due to the strong influence of the detonation front on the material. This influence seems to make the material yield more easily to the shear bands formation mechanism.

The mechanism by which local short shear bands sum up their lengths to the macroscopic value $\sqrt{2}\ d_{in}$ required for reaching break-up, is characteristic to ductile fracture in general and is not specific to the shaped charge jet. The formation of sliding tubes by the material between neighboring primary shear bands imposes, however, its order on this mechanism, that hopefully may be traced in some detail in the future.

REFERENCES

1. E. Hirsch, *A Formula for the Shaped Charge Jet Break-up Time,* Propellants, Explosives, Pyrotechnics 4, 89–94 (1979)
2. M. Mayseless, E. Hirsch, A. Lindenfeld and Y. Me-Bar, *Jet Tip and Appendix Characteristics Dependence on Liner Thickness in 60° Point Initiated Shaped-Charge,* 17th International Symposium on Ballistics, Midrand, South Africa, 2, 187 (1998)
3. M. Mayseless, E. Hirsch, A. Lindenfeld and A, Schwartz, *Effect of Explosive Energy on the Shaped Charge Jet Formation Characteristics,* 16th International Symposium on Ballistics, San Francisco, 13–27 Sept. Vol. 2, 411 (1997)
4. Part II in : D.L. Goodlin and T.R. Sharon. *ATTAC-Advanced Target/Threat Assessment Code Computer Program User's Manual Version 2.0,* Southwest Research Institute (Aug. 1998)
5. P.Y Chanteret and A. Lichtenberger, *About Varying Shaped Charge Liner Thickness,* 17th International Symposium on Ballistics, Midrand, South Africa. WM 31.Vol. 2, 365–372 (1998)
6. E. Hirsch, S. Chocron and G. Yossifon, *The Generalized Taylor Test and Strength-Flow Coupling in Ductile Metals,* 18th International Symposium on Ballistics, San Antonio, Texas, 924–93. 15–19 November (1999)
7. E. M. Pugh, R. J. Eichelberger and N. Rostoker, J. Appl. Phys. 23, 532 (1952)
8. F. Jamet, *Investigation of Shaped Charge Jets Using Flash X-Ray Diffraction,* 8th International Symposium on Ballistics, Orlando, Florida, October 23–25 (1984).
9. J.E. Backofen and E. Hirsch, *The Variable V_{pl} Model – A Strain Rate Sensitive Engineering Application of the V_{pl} Model,* Proceedings of the 13th International Symposium on Ballistics, Stockholm (1992) .
10. E. Hirsch, *The Natural Fragmentation of Thin Ductile Metal Shells,* 12th International Symposium on Ballistics, San Antonio, Texas, USA, Vol. 1, pp. 327-336 (1990)
11. E. Hirsch, *The Mixing of Liner Elements During Shaped Charge Jet Formation,* 16th International Symposium on Ballistics, San Francisco, California, Vol. 2, 293–302, Sep. 23–27 (1996)
12. E. Hirsch, *How does the Shaped Charge Jet Become Hollow?,* 13th International Symposium on Ballistics, Quebec, Canada (1993)
13. E. Hirsch, *Internal Shearing Direction During Shaped Charge Jet Formation and Break-up,* Propellants, Explosives, Pyrotechnics, 17,27–33 (1992)
14. Dov Chaiat, *Future P/M Materials for Kinetic Energy Penetrators and Shaped Charge Liners,* P/M in Defense Technology Seminar, 3–4 December 1986, David Taylor Naval Ship, Research and Development Center, Annapolis, Maryland, USA (1986)

15. E. Hirsch, *The Natural Mesh for Problems of Fragmenting Ductile Metal Shells*, 3rd International Conference on Hyperbolic Problems, Vol. II, 560–574. Uppsala, Sweden, June,11–15 (1990).
16. L. Zernow, E. D. Chapyak and S. J. Mosso, *A new 3D Computational Model for Shaped Charge Jet Breakup*, 16th International Symposium on Ballistics, San Francisco, CA, Vol. 2, 303–315, Sep. 23–28 (1996)
17. S.P. Timothy, *The Structure of Adiabatic Shear Bands in Metals*, F^3 Conference, Neve Ilan, Israel, Annals of the Israel Physical Society 8, p. 388 (Jan. 1986) .
18. J.E. Backofen, Private communication.

APPENDIX – STRESS BUILD UP TOWARD SHEAR BAND FORMATION

One may ask how such high stresses as mentioned in Table 1 can be obtained inside the material. To answer let's analyze how the flow stability is lost in a plastically flowing metal.

Stable plastic deformation involves microscopic sliding of dislocations at 45° with respect to the deformation direction [13]. In the example of a collapsing liner, the slide mainly occurs in those planes that are perpendicular to the liner surface and go through the axis of symmetry. Let's look at a cross section of the liner in such a plane. Let's call any slide of material toward the outer surface of the liner up and a slide toward the inner surface of the liner down. As long as the flow is stable the slides upward and downward balance each other. When stability is lost, this balance is locally lost. It means that regions appear where there is a bias toward one of these two main directions. These regions tend to grow by influencing neighboring sliding sites to adopt their bias direction.

At the beginning of this process there are many such growing regions distributed in the material randomly. Then, when they reach each other's influence range (collide) they will cancel each other's motion if being biased oppositely and mutually enhance their biased slide momentum if their slide motion is biased in the same direction. As this process continues the size of the regions grows and the biased slide motion at their boundaries also gains momentum, as described above. Finally, the boundaries of two oppositely biased regions meet, with amplitudes that are so large that the tension needed to mutually cancel their motion is too high for the material structural strength to hold and a shear band forms.

According to this description a shear band results from a collision between what we may call two oppositely biased sliding avalanches that had accumulated sufficient momentum. This can easily explain why the tension can reach in this case a value few times larger than the static yield tension.

Dynamic phenomena such as the above described avalanche can accumulate enough energy to form shear bands only when the strain rate is so high that their kinetic energy accumulation rate, more than compensates for their energy loss rate to heating of the material and to deforming it.